Assignment 1 – Introduction to LAMMPS

Sylvain Mortgat

June 19, 2025

1 FCC-Ag Relaxation

In this exercise, the goal is to determine the lowest energy configuration of a face-centered cubic (FCC) silver (Ag) crystal. This energy minimum is computed by relaxing both the atomic positions and the cell size. In Section 1.1, two models of atomic interactions are compared: the Lennard-Jones (LJ) potential and the Embedded Atom Method (EAM). Using both models, the energy and lattice constant are calculated after relaxation. The lattice constant is then varied around its optimal value. For each lattice constant, the energy of the crystal is computed without relaxation. This allows to establish the relationship between the total energy and the lattice constant. In Section 1.2, the bulk modulus of the crystal with LJ interactions is estimated by fitting the Birch-Murnaghan equation of state [1].

Packing Fraction of FCC-Ag The packing fraction of the FCC-Ag lattice is calculated as the ratio of the volume occupied by atoms to the total volume of the unit cell. Figure 1 depicts the conventional unit cell of an FCC lattice. In this structure, each atom has a radius r and occupies a volume $V_a = \frac{4}{3}\pi r^3$. Atoms at the corners contribute $\frac{1}{8}$ of their volume, while face-centered atoms contribute $\frac{1}{2}$. With 8 corner atoms and 6 face-centered atoms, the total occupied volume is $V_o = 8 \cdot \frac{V_a}{8} + 6 \cdot \frac{V_a}{2} = 4V_a$. To compute the volume of the unit cell, we first determine the lattice parameter a. For an FCC lattice, the diagonal of a face is equal to $4r$. Using the Pythagorean theorem, the face diagonal is $\sqrt{a^2 + a^2} = \sqrt{2}a$. Thus, $4r = \sqrt{2}a$, and solving for a gives $a = 2\sqrt{2}r$. The volume of the unit cell is then $V_c = (2\sqrt{2}r)^3$. The packing fraction of the FCC-Ag lattice is therefore

$$\frac{4V_a}{V_c} = \frac{16\pi r^3/3}{(2\sqrt{2}r)^3} = \frac{\sqrt{2}\pi}{6} \approx 0.74. \tag{1}$$

The same result can be derived from the primitive cell displayed in Figure 2. The primitive cell is spanned by the vectors $\vec{a}_1 = \frac{a}{2}(\vec{e}_x + \vec{e}_y)$, $\vec{a}_2 = \frac{a}{2}(\vec{e}_y + \vec{e}_z)$ and $\vec{a}_3 = \frac{a}{2}(\vec{e}_x + \vec{e}_z)$. Its volume is given by $V_p = |\vec{a}_1 \cdot \vec{a}_2 \times \vec{a}_3| = a^3/4$ and there is effectively one atom occupying the cell. Hence, the packing fraction is $\frac{V_a}{V_p} = \frac{4\pi r^3/3}{(2\sqrt{2}r)^3/4}$, which simplifies to the same expression as in Equation 1.

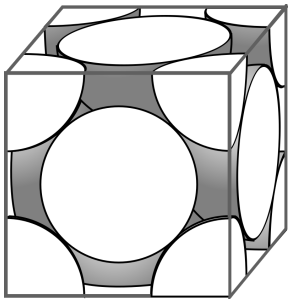

Figure 1: *Conventional unit cell of a FCC lattice [2].*

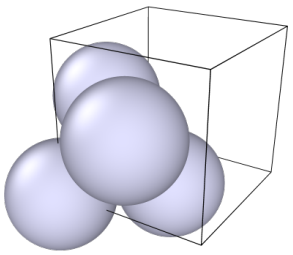

Figure 2: *Primitive cell of a FCC lattice.*

1.1 Comparison of Lennard-Jones and Embedded Atom Method Potentials

First, interactions between atoms of the lattice are modeled with the (12, 6) Lennard-Jones potential:

$$V(r) = 4\varepsilon\left[\left(\frac{\sigma}{r}\right)^{12} - \left(\frac{\sigma}{r}\right)^{6}\right] =: \frac{A}{r^{12}} - \frac{B}{r^6}, \tag{2}$$

where r represents the interatomic distance, ε [eV] is the potential depth, and σ [Å] is the van der Waals radius at which the potential is zero ($V(\sigma) = 0$). The last equality in Equation 2 defines the

constants $A := 4\varepsilon\sigma^{12}$ and $B := 4\varepsilon\sigma^{6}$. This potential consists of a short-range repulsive term $\propto r^{-12}$ arising from the Pauli exclusion principle and an attractive term $\propto r^{-6}$ that models van der Waals interactions.

In the simulations, the Lennard-Jones (LJ) potential parameters are set to $\varepsilon = 0.341$ eV and $\sigma = 2.648$ Å, with a cutoff radius of 20 Å. For the EAM simulation, we use a model provided in [3]. For both interaction models, the lattice is initialized with a lattice constant of 6 Å. Energy minimization is performed with an energy tolerance of 10^{-6} and a force tolerance of 10^{-8} eV/Å. The results of the energy minimization, including the total energy and optimized lattice constant for both models, are summarized in Table 1.

Model	E_{tot} [eV]	a_{opt} [Å]
Lennard-Jones	−11.715	4.083
Embedded Atom Method	−11.400	4.090

Table 1: *Comparison of the total energy (E_{tot}) and optimized lattice constant (a_{opt}) for FCC-Ag after relaxation using Lennard-Jones and Embedded Atom Method interactions.*

Then, the total energy is evaluated for various lattice parameters around the optimal values reported in Table 1 for both the LJ and EAM models. The results, presented in Figure 3, show that in both cases, the energy varies as a function of the lattice constant in a parabolic manner. However, the Lennard-Jones potential leads to a steeper curve with a deeper minimum compared to the EAM model. The disparity in total energy magnitudes between LJ and EAM is expected, as the two models fundamentally differ in their representation of atomic interactions. Consequently, absolute energy values are not directly comparable across models. Instead, the important quantity is the lattice constant at the energy minimum. The optimal lattice constant obtained from the EAM model remains consistent with the value in Table 1. For the LJ potential, a slightly different value of 4.082 Å is observed. Both values are close to the experimental lattice constant of 4.09 Å[4]. The EAM shows excellent agreement. The relative error for LJ interactions is about 0.2%, while for EAM it is negligible.

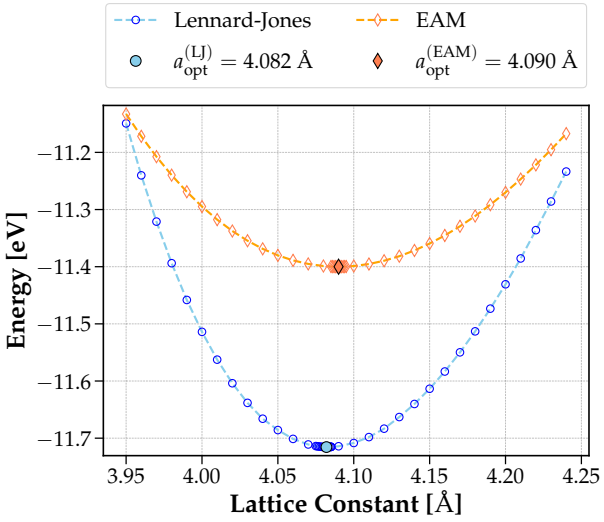

Figure 3: *Comparison of the total energy as a function of the lattice parameter for the Lennard-Jones potential and the Embedded Atom Model. The lattice constants corresponding to the energy minima are close to the experimental value of 4.09Å[4].*

1.2 Bulk Modulus Estimation

The bulk modulus is estimated using Lennard-Jones interactions by fitting the Birch-Murnaghan isothermal equation of state [1] around the equilibrium lattice constant:

$$E(V) = E_0 + \left(\frac{9}{8}\right) B_0 V_0 \left[\left(\frac{V_0}{V}\right)^{2/3} - 1\right]^2 + \left(\frac{9}{16}\right) B_0 V_0 \left(B_0' - 4\right) \left[\left(\frac{V_0}{V}\right)^{2/3} - 1\right]^3. \tag{3}$$

Here, B_0 is the bulk modulus, B_0' its derivative, V the cell volume, V_0 the equilibrium volume, and E_0 the equilibrium energy. The parameters B_0, B_0', V_0, and E_0 are determined by performing a nonlinear

least-squares fit using the function `scipy.optimize.curve_fit`. The 95% confidence intervals for these parameters are calculated using a t-statistic.

The fitted values obtained are: $B_0 = (1.387 \pm 0.002)\,\text{eV} \cdot \text{Å}^{-3}$, $E_0 = -(11.7156 \pm 0.0002)\,\text{eV}$, $V_0 = (68.067 \pm 0.006)\,\text{Å}^3$, and $B_0' = 7.93 \pm 0.07$. Figure 4 illustrates the fit to the energy-volume data using the optimized parameters. To express the bulk modulus in GPa, the appropriate unit conversion factor is applied: $1\,\text{Pa} = 1\,\text{J} \cdot \text{m}^{-3}$, $1\,\text{J} = 1.602176634 \cdot 10^{-19}\,\text{eV}$ and $1\,\text{Å} = 10^{-10}\,\text{m}$. Using these, we find $B_0 = (222.3 \pm 0.3)$ GPa. The obtained value is of the correct order of magnitude but represents a significant overestimate compared to experimental data. Literature values report $B_0 = 101$ GPa experimentally [4] and 128 GPa from theoretical calculations [5]. For comparison, the same fitting procedure is applied to the data obtained using the EAM potential. In this case, the estimated bulk modulus is (103.55 ± 0.02) GPa, which shows significantly better agreement with both experimental and theoretical values.

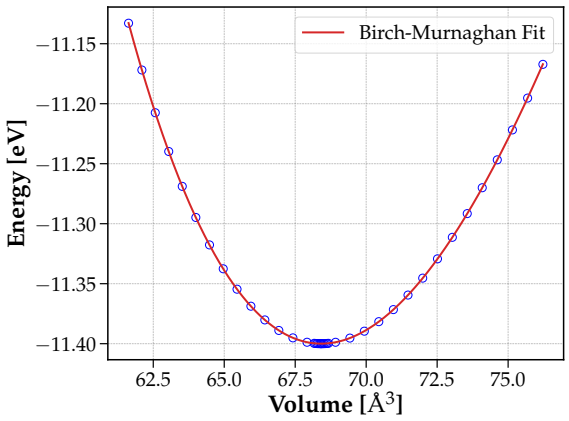

Figure 4: *Nonlinear least-squares fit of the Birch-Murnaghan equation of state to the energy-volume data. The bulk modulus is determined to be* $B_0 = (222.3 \pm 0.3)$ GPa.

2 Vacancy Formation Energy

This exercise focuses on calculating the vacancy formation energy in a FCC-Ag crystal. In Section 2.1, the convergence of the vacancy formation energy with respect to supercell size is investigated using the Lennard-Jones (LJ) potential. The energy is computed both with and without atomic relaxation to assess the impact of structural relaxation on the vacancy formation energy. In Section 2.2, the results obtained using the LJ potential are compared with those from the EAM potential. Finally, the computed values are analyzed against the experimental vacancy formation energy of FCC-Ag to evaluate the accuracy of the employed empirical potentials.

2.1 Vacancy Formation Energy with LJ Interactions

The vacancy formation energy, $E_{\text{f,v}}$, is defined as the energy required to remove an atom from the lattice and place it at infinity. It is given by

$$E_{\text{f,v}} = E_{i,N-1} - \left(\frac{N-1}{N}\right) E_{i,N}, \tag{4}$$

where $E_{i,N-1}$ and $E_{i,N}$ are the energies of the supercell with $N-1$ and N atoms, respectively. To compute $E_{\text{f,v}}$, FCC-Ag supercells are constructed by replicating the conventional unit cell $n \times n \times n$ times in the x, y, and z directions, with n ranging from 1 to 14. The corresponding number of atoms N in each supercell is listed in Table 2. The lattice constant is defined with the optimal value found in Figure 3. A vacancy is introduced by removing one atom from the supercell. The use of supercells ensures that periodic boundary conditions do not artificially amplify interactions between the vacancy and its periodic images. By increasing n, the distance between vacancies grows, reducing finite-size effects. This allows $E_{\text{f,v}}$ to converge to its bulk value as the supercell size becomes sufficiently large, as visualized for representative cell sizes in Figure 10 in the Appendix A. Convergence of $E_{\text{f,v}}$ is determined by requiring the absolute value difference between the energy for a given supercell size and the energy of the largest supercell ($n = 14$), denoted $\Delta E_{\text{f,v}}$, to fall below a threshold of 10^{-5} eV.

n	1	2	3	4	5	6	7	8	9	10	11	12	13	14
N	4	32	108	256	500	864	1 372	2 048	2 916	4 000	5 324	6 912	8 788	10 976

Table 2: *Number of atoms N in FCC-Ag supercells for different scaling factors n, with n representing the number of of cell repetitions along each Cartesian direction.*

For LJ interactions, the vacancy formation energy $E_{f,v}$ converges to 2.87853 eV (fixed lattice) and 2.87858 eV (relaxed lattice) for supercells with $n \geq 3$, as shown in Figure 5(a). The negligible difference (0.00005 eV) between fixed and relaxed cases indicates atomic relaxation minimally impacts LJ-based calculations. The LJ-derived vacancy formation energy overestimates the experimental value of 1.11 eV by 160%. This highlights its limitations for metallic systems. This inaccuracy is further reflected in the ratio of vacancy formation energy to cohesive energy, which equals 1 for LJ interactions (this is a theoretical artifact of pair-potential approximations) compared to the experimental ratio of 0.39 [6].

2.2 Comparison with EAM

The EAM potential demonstrates a different convergence behavior as shown in Figure 5(b). It requires $n \geq 3$ for fixed lattices but $n \geq 13$ for relaxed configurations. The converged $E_{f,v}$ values of 0.965 eV (fixed) and 0.968 eV (relaxed) align better with the experimental value of 1.11 eV, with a 13% relative error. The vacancy-to-cohesive energy ratio (0.339 for fixed, 0.340 for relaxed) is also more accurate with respect to the reference value (13% relative error).

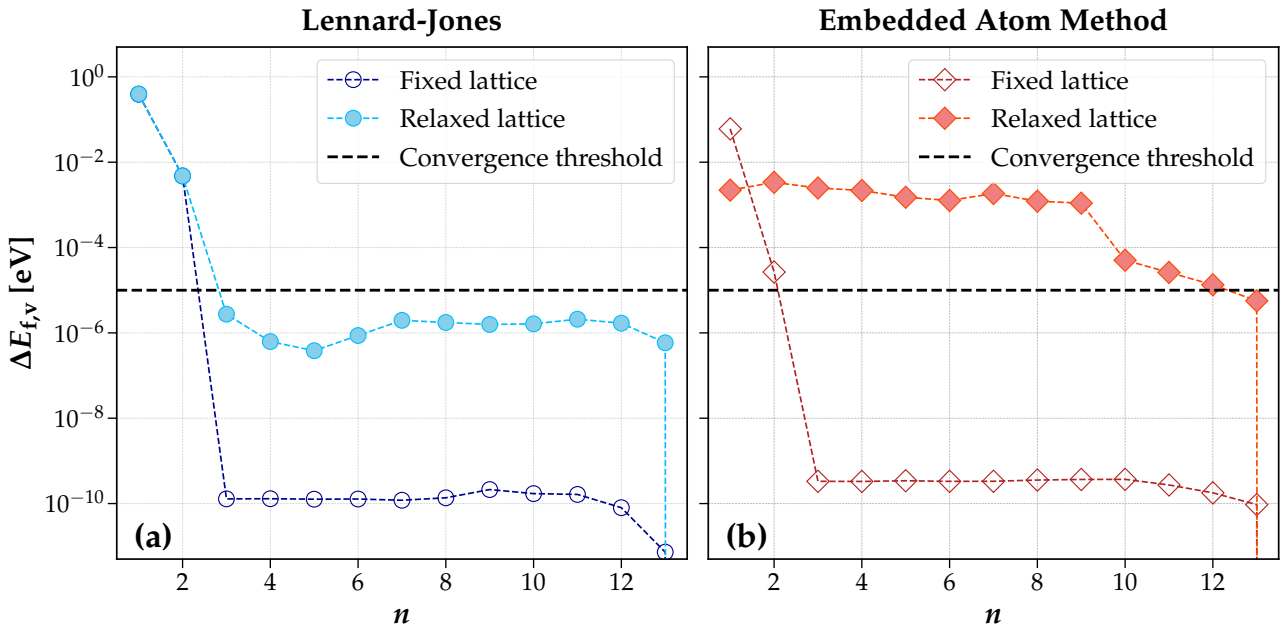

Figure 5: *Convergence of the vacancy formation energy difference, $\Delta E_{f,v}$, between the energy for a given supercell size and the energy of the largest supercell, comparing* ***(a)*** *LJ interactions and* ***(b)*** *EAM potential. Results are shown for fixed and relaxed lattices. The horizontal black dashed line indicates the convergence threshold of 10^{-5} eV. For the LJ potential, convergence is achieved for $n \geq 3$, while for the EAM potential, the fixed-lattice case converges at $n \geq 3$ and the relaxed-lattice case at $n \geq 13$.*

3 Surface Energy Calculation

This exercise focuses on determining the surface energy of the FCC-Ag (100) surface using the Lennard-Jones potential. First, the concept of surface energy is introduced, and the methodology for constructing slab supercells with vacuum separation is described. The surface energy is computed for different slab thicknesses and vacuum sizes to ensure convergence. Then the convergence of the computed surface energy is analyzed, and the effect of atomic relaxation is discussed.

Surface Energy The surface energy, denoted γ_{slab} [eV/Å^2], is defined as the cost of creating a termination of the bulk crystal along a crystallographic plane. For a supercell model containing slabs with two equivalent surfaces, it is given by

$$\gamma_{\text{slab}} = \frac{E_{\text{slab}} - NE_{\text{bulk}}}{2A_{\text{slab}}}. \tag{5}$$

Here, E_{slab} and E_{bulk} are the total energy of the slab and the bulk energy per atom, respectively. N is the number of atoms in the slab, and A_{slab} is the surface area of a single interface. The denominator includes a factor of 2 because periodic boundary conditions automatically generate two equivalent surfaces.

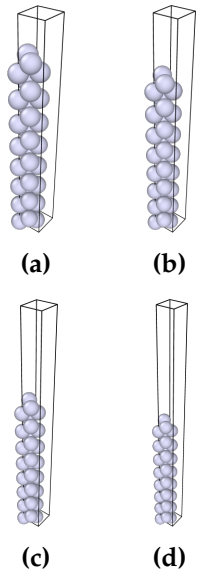

Figure 6: *Visualization of a supercell containing 8 repetitions of the FCC-Ag unit cell with varying vacuum thickness:* ***(a)*** *1 layer,* ***(b)*** *2 layers,* ***(c)*** *4 layers, and* ***(d)*** *6 layers.*

Methodology Slab supercells are constructed by varying the number of unit cell repetitions in the slab (n_{layers}) and vacuum region (n_{vac}) from 1 to 8. Converging the vacuum thickness is important to ensure that the periodic images of the slab do not interact with each other. Similarly, slab thickness must be large enough to avoid interaction between the two surfaces of one slab. This also ensures that the central layers exhibit true bulk-like properties. Figure 6 illustrates representative supercells with 8 unit cell repetitions and vacuum thicknesses of $n_{\text{vac}} = 1$, 2, 4, and 6. Surface energy calculations are performed for all $(n_{\text{layers}}, n_{\text{vac}})$ combinations using single-point energy evaluations without structural relaxation. This allows to isolate the energy cost of creating an ideal surface. If relaxation were allowed, surface atoms would rearrange to lower the total energy and reduce γ_{slab}. Keeping atoms fixed ensures that only the intrinsic surface energy is measured, without taking energy changes from atomic rearrangements into account. To assess convergence, a reference surface energy value of $\gamma_{\text{slab}} = 0.15474107$ eV/Å^2 is computed for a highly converged supercell with $n_{\text{layers}} = n_{\text{vac}} = 100$. A threshold of 10^{-5} eV is adopted, requiring the absolute difference between γ_{slab} values obtained for smaller $(n_{\text{layers}}, n_{\text{vac}})$ combinations and this reference to fall below the threshold. This quantity is denoted $\Delta\gamma_{\text{slab}}$.

Results Figure 7 shows the computed surface energy values γ_{slab} as a function of slab thickness and vacuum thickness. Interestingly, a convergence symmetry in n_{layers} and n_{vac} is observed. The convergence of γ_{slab} is analyzed first for fixed n_{vac} with varying n_{layers} (Fig. 8(a)), and then for fixed n_{layers} with varying n_{vac} (Fig. 8(b)). In both cases, the convergence behavior is similar, as expected from the symmetry observed in Figure 7, and convergence to the reference value is achieved for $n_{\text{layers}}, n_{\text{vac}} \geq 5$. This value is positive, which makes sense as this indicates that forming a surface is energetically unfavorable (it requires energy). If γ_{slab} were negative, surfaces would spontaneously form, and the material would disintegrate to maximize surface area.

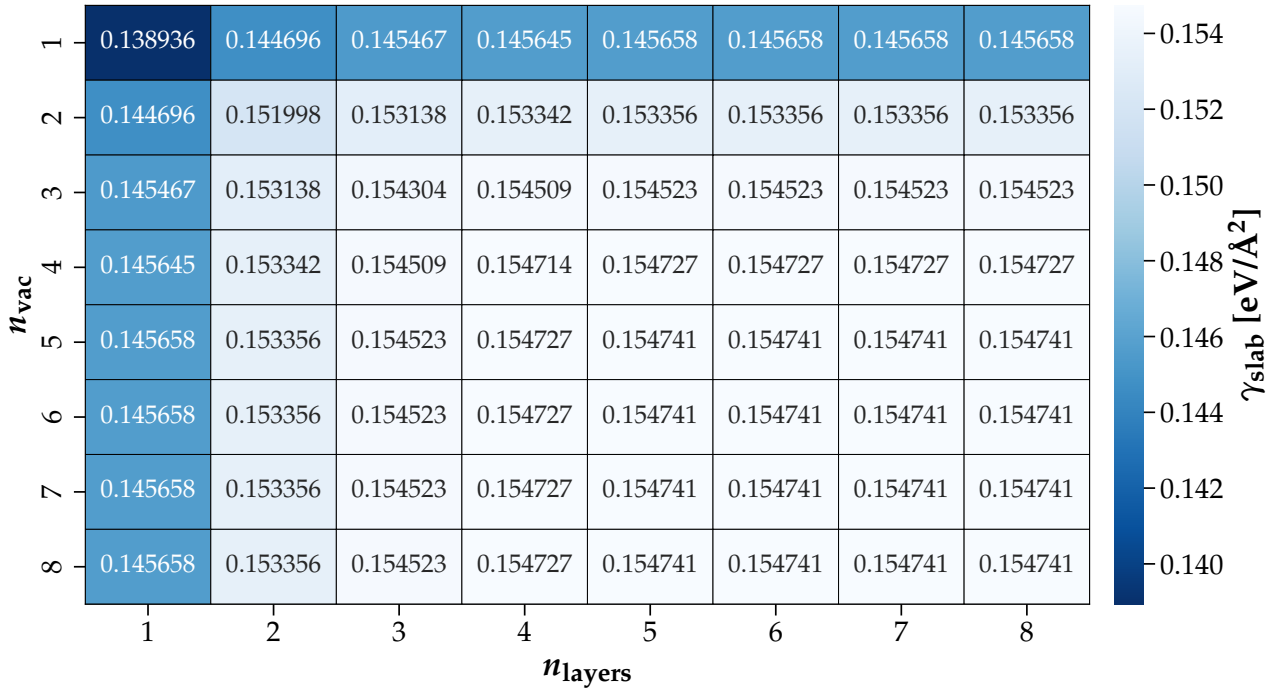

Figure 7: *Surface energy values γ_{slab} computed for varying slab thickness (n_{layers}) and vacuum thickness (n_{vac}). For fixed n_{layers}, γ_{slab} converges for $n_{vac} \geq 5$; similarly, for fixed n_{vac}, convergence is achieved for $n_{layers} \geq 5$. Notably, the convergence exhibits symmetry in n_{layers} and n_{vac}.*

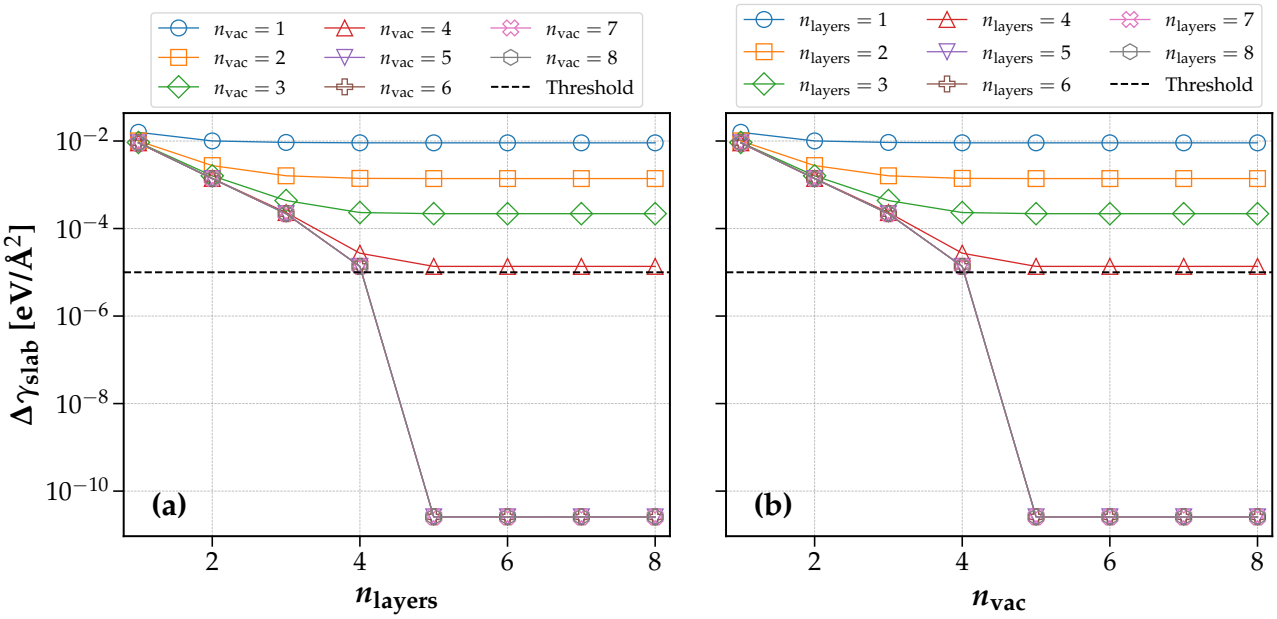

Figure 8: *Convergence of the surface energy error $\Delta\gamma_{slab}$, defined as the absolute difference between computed values and the reference γ_{slab} at $n_{\text{layers}} = n_{\text{vac}} = 100$. **(a)** Convergence behavior for varying n_{layers} with fixed n_{vac}. **(b)** Convergence for varying n_{vac} with fixed n_{layers}. In both cases, convergence is achieved for $n \geq 5$.*

4 Choice of Empirical Potentials

The Lennard-Jones potential is well-suited for modeling noble gases (e.g., Ar), simple fluids, and systems dominated by isotropic van der Waals interactions, where many-body effects are negligible. In contrast, the Embedded Atom Method works well for metallic systems as it captures many-body interactions through electron density embedding. But neither LJ nor EAM are reliable for materials with directional bonding, these two methods are not really appropriate for covalent systems, ionic crystals, or scenarios requiring explicit quantum mechanical effects. As an alternative, the Modified Embedded Atom Method (MEAM) extends EAM by incorporating angular dependencies. This enables a more accurate modeling of anisotropic structures. MEAM performs better in systems with directional bonding, such as surface reconstructions in silicon or mechanical properties of steel alloys.

5 Minimum of the Lennard-Jones Potential

The minimum of the Lennard-Jones potential, denoted r_0, is determined by setting the derivative of the potential with respect to r to zero. Starting from Equation (2),

$$\left.\frac{\mathrm{d}V}{\mathrm{d}r}\right|_{r=r_0} = -12Ar_0^{-13} + 6Br_0^{-7} \stackrel{!}{=} 0. \tag{6}$$

This leads to $12Ar_0^{-6} = 6B$, which simplifies to $r_0 = \left(\frac{2A}{B}\right)^{1/6} = 2^{1/6}\sigma$, where the last equality follows from the definitions of A and B. In Section 1, the Lennard-Jones parameters were defined as $\varepsilon = 0.341$ eV and $\sigma = 2.648$ Å. Substituting these into the previous expression for r_0 gives $r_0 \approx 2.972$ Å. This result can be compared to the nearest-neighbor distance found by relaxing the lattice in Section 1.1, where the optimal lattice constant was determined as $a_{\mathrm{opt}} = 4.082$ Å, corresponding to a nearest-neighbor distance of $r_{\mathrm{opt}} = a_{\mathrm{opt}}/\sqrt{2} \approx 2.886$ Å. The discrepancy between r_0 and r_{opt} arises because r_0 minimizes the energy of an isolated atomic pair, whereas the FCC lattice equilibrium accounts for all pairwise interactions within the structure.

6 Properties of the CuAu L1$_0$ Binary Phase

In this exercise, the L1$_0$ CuAu binary alloy is modeled using empirical potentials to determine its structural properties. In Section 6.1 Lennard-Jones parameters for elemental Cu and Au are extracted from the literature [7] and combined via geometric mixing rules [8] to describe cross-species interactions. Equilibrium lattice parameters are then optimized for given initial conditions, and the final cell geometries are compared to experimental references. The same optimization is performed using a pre-fitted EAM potential. This enables a direct comparison between the two models. Finally, few more general aspects of the EAM potential are discussed in Section 6.2.

6.1 Equilibrium Lattice Parameters

The CuAu L1$_0$ Binary Phase The L1$_0$ phase of the CuAu binary alloy adopts a tetragonal structure (Fig. 9). The primitive lattice vectors are given by

$$\vec{a}_1 = a\,\vec{e}_x, \quad \vec{a}_2 = a\,\vec{e}_y, \quad \vec{a}_3 = c\,\vec{e}_z,$$

and the basis vectors by

$$\vec{b}_{\mathrm{Cu}} = \vec{0}, \quad \vec{b}_{\mathrm{Au}} = \frac{1}{2}(\vec{a}_1 + \vec{a}_2 + \vec{a}_3).$$

Thus, the unit cell volume is $V = a^2 c$ [10].

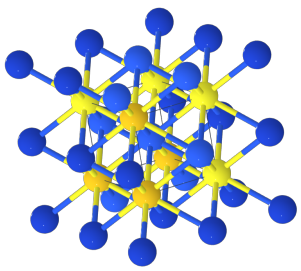

Figure 9: *CuAu L1$_0$ binary phase with $a = c$ [9] .*

Methodology & Results The equilibrium lattice parameters are determined by relaxing the lattice from various initial configurations. In the Lennard-Jones approach, the elemental parameters are taken from the literature [7], with $\varepsilon_{\mathrm{Au}} = 0.22941$ eV, $\varepsilon_{\mathrm{Cu}} = 0.20476$ eV, $\sigma_{\mathrm{Au}} = 2.62901$ Å, and $\sigma_{\mathrm{Cu}} = 2.33050$ Å. Cross-species interactions are modeled using the standard geometric mixing rules [8], which yield

$$\varepsilon_{\mathrm{CuAu}} = \sqrt{\varepsilon_{\mathrm{Cu}}\varepsilon_{\mathrm{Au}}} = 0.21673 \text{ eV} \quad \text{and} \quad \sigma_{\mathrm{CuAu}} = \sqrt{\sigma_{\mathrm{Cu}}\sigma_{\mathrm{Au}}} = 2.47526 \text{ Å}.$$

A cut-off distance of 10 Å is applied for the LJ interactions. Additionally, a pre-fitted EAM potential [11] is employed to optimize the lattice parameters. The final cell geometries obtained from both models are listed in Table 3. Initial conditions seem to play a significant role in determining the equilibrium lattice parameters. When the cell is initialized with equal lattice constants ($a_{\mathrm{i}} = c_{\mathrm{i}}$), the symmetry is maintained during relaxation. In contrast, for cases with $a_{\mathrm{i}} \neq c_{\mathrm{i}}$, although the relative ordering is preserved (i.e., if $a_{\mathrm{i}} > c_{\mathrm{i}}$, then $a_{\mathrm{f}} > c_{\mathrm{f}}$, and vice versa), the final values may differ. In most simulations, the relaxed cell volume converges to approximately 30 Å^3, but notably, the last two cases exhibit a large deviation despite the energy minimization reaching an energy tolerance of 10^{-10}. The LJ potential yields lattice parameters for the initialization $a_{\mathrm{i}} = 3$ Å, $c_{\mathrm{i}} = 5$ Åthat closely match reference values ($a = 2.80$ Å, $c = 3.67$ Å) from [12], with relative errors of only 1% for a_{f} and 2.5% for c_{f}. In contrast, Modified Embedded Atom Method simulations conducted in [13] predict a substantially expanded unit cell ($a = 3.96$ Å, $c = 3.67$ Å, $V = 57.75$ Å^3) that deviate from both the LJ and EAM results obtained in this present work.

Initial Conditions			LJ Results			EAM Results		
a_{i} [Å]	c_{i} [Å]	V_{i} [Å^3]	a_{f} [Å]	c_{f} [Å]	V_{f} [Å^3]	a_{f} [Å]	c_{f} [Å]	V_{f} [Å^3]
3	3	27	3.02	3.02	27.41	3.07	3.07	28.99
6	6	216	3.06	3.06	28.78	3.07	3.07	28.99
3	5	45	2.77	3.76	28.67	2.57	4.28	28.22
5	3	75	3.23	2.78	29.06	3.82	2.29	33.58
5	7	175	2.94	4.15	36.00	3.01	4.21	37.99
7	5	245	5.56	2.96	91.09	3.46	2.47	29.59

Table 3: *Comparison of optimized lattice parameters (lattice constants a, c and unit cell volume V) for a CuAu system under different initial conditions. Results are obtained using LJ and EAM potentials.*

6.2 EAM potential for a FCC-Au crystal

In the EAM framework, the total energy of a system is expressed as

$$E_{\mathrm{tot}} = \sum_i F(\rho_i) + \frac{1}{2}\sum_{\substack{i,j \\ j\neq i}} \phi(r_{ij}). \tag{7}$$

The total energy is partitioned into a many-body embedding term and a pairwise interaction term. The embedding function $F(\rho_i)$ represents the energy required to insert atom i into the local electron density ρ_i, which is generated by the surrounding atoms. The electron density at atom i is given by

$$\rho_i = \sum_{j\neq i} f(r_{ij}), \tag{8}$$

with $f(r_{ij})$ denoting the contribution to the electron density at atom i from atom j, and r_{ij} representing the distance between atoms i and j. The two-body potential $\phi(r_{ij})$ accounts for the direct interactions

between pairs of atoms. This formulation makes $F(\rho_i)$ inherently a many-body contribution. While ρ_i itself is a linear superposition of pairwise terms $f(r_{ij})$, the embedding energy $F(\rho_i)$ depends nonlinearly on the total ρ_i. This nonlinearity ensures that $F(\rho_i)$ cannot be expressed as a sum of individual pair interactions. Instead, it captures the collective influence of the entire atomic environment surrounding atom i. For instance, coordination effects are taken into account.

Here, a FCC-Au crystal is considered using the EAM as detailed in [14]. In that work, the form of both the electron density function f and the two-body potential ϕ are specified. They are assumed to arise primarily from nearest neighbor interactions. This is justified by the fact that nearest neighbor contributions are dominant [15]. The electron density contribution from an atom at a distance r is given by

$$f(r) = f_e \, e^{-\beta\left(\frac{r}{r_e}-1\right)}, \tag{9}$$

where f_e, β, and r_e are parameters characteristic of the material. The embedding function $F(\rho)$ is obtained by fitting the model to a universal equation of state:

$$F(\rho) = -E_c \left\{1 - \ln\left[\left(\frac{\rho}{\rho_e}\right)^{\alpha/\beta}\right]\right\}\left(\frac{\rho}{\rho_e}\right)^{\alpha/\beta} - 6\phi_e\left(\frac{\rho}{\rho_e}\right)^{\gamma/\beta}. \tag{10}$$

The values of the parameters for Au are tabulated in Table 1 of [14]. Assuming only nearest-neighbor contributions in Equation 8, the electron density ρ_i can be explicitly derived for the FCC lattice. From Section 1, the nearest-neighbor distance in FCC is $a/\sqrt{2}$, where a is the lattice constant. Substituting the electron density function $f(r)$ from Equation 9, the local electron density becomes

$$\rho_i = \sum_{\langle i,j\rangle} f(r_{ij}) = 12\, f(a/\sqrt{2}) = 12 f_e \, e^{-\beta\left(a/(\sqrt{2}r_e)-1\right)}, \tag{11}$$

where $\sum_{\langle i,j\rangle}$ denotes summation over nearest neighbors, and the prefactor 12 arises from the FCC coordination number.

Total energy of a monoatomic crystal In a monoatomic crystal with N atoms, the equivalence of all atomic sites implies a uniform electron density $\rho_i \equiv \rho$. Therefore, the embedding function $F(\rho)$ becomes site-independent. The energy of an individual atom i is expressed as

$$E_i = F(\rho) + \sum_{\substack{j=1 \\ j\neq i}}^{N} \phi(r_{ij}). \tag{12}$$

Summing E_i over all atoms yields the total energy, but pairwise potentials $\phi(r_{ij})$ are double-counted. To correct this, the total energy becomes

$$E_{\text{tot}} = \sum_{i=1}^{N} E_i - \frac{1}{2}\sum_{i=1}^{N}\sum_{\substack{j=1 \\ j\neq i}}^{N} \phi(r_{ij}) = \sum_{i=1}^{N}\left[F(\rho) + \frac{1}{2}\sum_{\substack{j=1 \\ j\neq i}}^{N}\phi(r_{ij})\right]. \tag{13}$$

Given the crystal's periodicity, each atom's environment is identical. This allows the summation over neighbors to be expressed uniformly. The total energy simplifies to

$$E_{\text{tot}} = N\left[F(\rho) + \frac{1}{2}\sum_{m}\phi(r_m)\right] =: NE, \tag{14}$$

where m enumerates all neighboring interactions. The last equality defines the per-atom energy E.

References

[1] Tomoo Katsura and Yoshinori Tange. "A Simple Derivation of the Birch–Murnaghan Equations of State (EOSs) and Comparison with EOSs Derived from Other Definitions of Finite Strain". In: *Minerals* 9.12 (2019). ISSN: 2075-163X. DOI: 10.3390/min9120745. URL: https://www.mdpi.com/2075-163X/9/12/745.

[2] Wikimedia Commons. *File:Cubique a faces centrees atomes par maille.svg — Wikimedia Commons, the free media repository*. [Online; accessed 17-March-2025]. 2024. URL: https://commons.wikimedia.org/w/index.php?title=File:Cubique_a_faces_centrees_atomes_par_maille.svg&oldid=871764596.

[3] S. M. Foiles, M. I. Baskes, and M. S. Daw. "Embedded-atom-method functions for the fcc metals Cu, Ag, Au, Ni, Pd, Pt, and their alloys". In: *Phys. Rev. B* 33 (12 June 1986), pp. 7983–7991. DOI: 10.1103/PhysRevB.33.7983. URL: https://link.aps.org/doi/10.1103/PhysRevB.33.7983.

[4] Charles Kittel. *Introduction to Solid State Physics*. 8th ed. Wiley, 2004. ISBN: 9780471415268. URL: http://www.amazon.com/Introduction-Solid-Physics-Charles-Kittel/dp/047141526X/ref=dp_ob_title_bk.

[5] Jianjun Xie et al. "First-principles calculation of the thermal properties of silver". In: *Phys. Rev. B* 59 (2 Jan. 1999), pp. 965–969. DOI: 10.1103/PhysRevB.59.965. URL: https://link.aps.org/doi/10.1103/PhysRevB.59.965.

[6] Murray S. Daw, Stephen M. Foiles, and Michael I. Baskes. "The embedded-atom method: a review of theory and applications". In: *Materials Science Reports* 9.7 (1993), pp. 251–310. ISSN: 0920-2307. DOI: https://doi.org/10.1016/0920-2307(93)90001-U. URL: https://www.sciencedirect.com/science/article/pii/092023079390001U.

[7] Hendrik Heinz et al. "Accurate Simulation of Surfaces and Interfaces of Face-Centered Cubic Metals Using 12-6 and 9-6 Lennard-Jones Potentials". In: *The Journal of Physical Chemistry C* 112.44 (2008), pp. 17281–17290. DOI: 10.1021/jp801931d. URL: https://doi.org/10.1021/jp801931d.

[8] DL_Software Digital Guide. *Lennard-Jones Mixing Rules*. 2025. URL: https://dl-sdg.github.io/RESOURCES/FORCE_FIELD/ff10.html.

[9] The Materials Project. "Materials Data on CuAu by Materials Project". In: (July 2020). DOI: 10.17188/1263147. URL: https://next-gen.materialsproject.org/materials/mp-522.

[10] Michael J. Mehl et al. "The AFLOW Library of Crystallographic Prototypes: Part 1". In: *Computational Materials Science* 136 (2017), S1–S828. ISSN: 0927-0256. DOI: https://doi.org/10.1016/j.commatsci.2017.01.017. URL: https://www.sciencedirect.com/science/article/pii/S0927025617300241.

[11] Gregory Grochola, Salvy P. Russo, and Ian K. Snook. "On fitting a gold embedded atom method potential using the force matching method". In: *The Journal of Chemical Physics* 123.20 (Nov. 2005), p. 204719. ISSN: 0021-9606. DOI: 10.1063/1.2124667. eprint: https://pubs.aip.org/aip/jcp/article-pdf/doi/10.1063/1.2124667/15376793/204719_1_online.pdf. URL: https://doi.org/10.1063/1.2124667.

[12] E. Bjerkelund et al. "Lattice Parameters of the CuAu(I) Phase". In: *Acta Chemica Scandinavica* 21 (1967), pp. 2900–2902. DOI: 10.3891/acta.chem.scand.21-2900.

[13] Zhong-Liang Lin et al. "Atomistic simulation of point defects in L10-type CuAu ordered alloy". In: *physica status solidi (b)* 248.4 (2011), pp. 897–903. DOI: https://doi.org/10.1002/pssb.201046386. URL: https://onlinelibrary.wiley.com/doi/abs/10.1002/pssb.201046386.

[14] R. A. Johnson. "Alloy models with the embedded-atom method". In: *Phys. Rev. B* 39 (17 June 1989), pp. 12554–12559. DOI: 10.1103/PhysRevB.39.12554. URL: https://link.aps.org/doi/10.1103/PhysRevB.39.12554.

[15] R. A. Johnson. "Analytic nearest-neighbor model for fcc metals". In: *Phys. Rev. B* 37 (8 Mar. 1988), pp. 3924–3931. DOI: 10.1103/PhysRevB.37.3924. URL: https://link.aps.org/doi/10.1103/PhysRevB.37.3924.

A Additional Figure

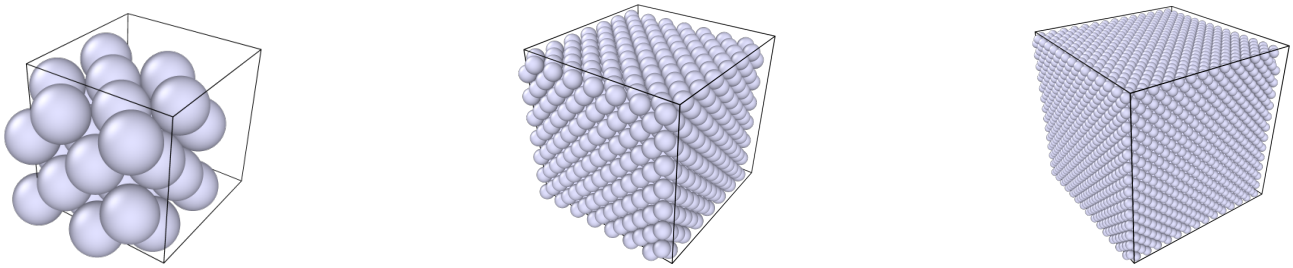

(a) **(b)** **(c)**

Figure 10: *Visualization of FCC-Ag supercells used for vacancy formation energy calculations:* ***(a)*** $2 \times 2 \times 2$ *supercell* ($N = 32$ *atoms),* ***(b)*** $7 \times 7 \times 7$ *supercell* ($N = 1\,372$ *atoms), and* ***(c)*** $14 \times 14 \times 14$ *supercell* ($N = 10\,976$ *atoms).*